# Supplementary Information
# DFT insights into nano-Au/carbon nitride: Potent CO oxidation facilitated by weak metal-support interaction

Milad Behroozi and Esmail Doustkhah*
*Chemistry Department, Faculty of Engineering and Natural Sciences, Istinye University, Istanbul* 34396 *Türkiye. and*
*Clean Energy Research Center (TEAM), Istinye University, Sariyer, Istanbul* 34396 *Türkiye.*

M. Hussein N. Assadi†
*RIKEN Center for Emergent Matter Science (CEMS), Wako, Saitama* 351−0198 *Japan and*
*Chemistry Department, Faculty of Engineering and Natural Sciences, Istinye University, Istanbul* 34396 *Türkiye.*
(Dated: December 15, 2025)

## SUPPLEMENTARY ANALYSIS

### Supplementary Table

TABLE S1. The lattice parameters of the optimised $Au_x@C_3N_2$ supercells.

| Configuration | $a$ (Å) | $b$ (Å) | $c$ (Å) | $\alpha$ | $\beta$ | $\gamma$ |
|---|---|---|---|---|---|---|
| 1-Layer | 10.169 | 5.069 | 33.681 | 89.48° | 85.98° | 89.98° |
| 2-Layer | 10.217 | 5.023 | 53.929 | 89.51° | 85.97° | 89.98° |
| 4-Layer | 10.249 | 4.954 | 60.002 | 89.94° | 90.05° | 90.06° |
| 8-Layer | 10.171 | 5.085 | 70.585 | 90.00° | 90.00° | 90.00° |

### Supplementary Figures

Au is renowned for its catalytic activity, even at uncommonly low temperatures ($\sim$ 203 K), in oxidising CO to $CO_2$ [S1]. This reaction is essential in various industrial processes, particularly automotive catalytic converters and gas sensors. The precise mechanism by which gold catalyses this reaction is still an active research area [S2]. In principle, sufficient charge transfer from the catalyst to the CO and $O_2$ molecules is indispensable for any catalytic CO oxidation to be effective. We demonstrate the criticality of such charge transfer in Figure S1a and b, where we can see that for both CO and $O_2$, the lowest energy orbitals that can still accept electrons, presumably from the catalyst, have antibonding $\pi^*_{2p}$ nature. Upon the adsorption of CO and $O_2$ molecules onto the Au surface, given the high lability of 5d electrons at the surface, their transfer into the antibonding $\pi^*_{2p}$ orbital weakens the O−O and C−O bonds. The case for $O_2$ is particularly acute because the weakening of the bond results in the formation of chemisorbed oxygen species ($O^\bullet$) [S3], which would react with the adsorbed CO to form $CO_2$. The resulting $CO_2$ desorbs relatively easily from the catalyst surface because its lowest available orbital is too high to retain the charge from Au [S4] (also schematically shown in Figure S1c), thus being released and freeing up active sites for further CO oxidation. In other words, Au's sizable 5d population, minimal interaction with the substrate, which preserves its catalytically labile and active electrons, and resistance to $CO_2$ poisoning render it an ideal sub-nano catalyst.

Crystal orbital hamilton population (COHP) identifies bonding, non-bonding, and antibonding interactions between specific atomic pairs by partitioning the band-structure energy into Hamilton-matrix-weighted contributions. Negative COHP values reveal stabilising bonding interactions, whilst positive values indicate destabilising antibonding states, allowing quantification of interaction strength and structural preferences. Integrating the COHP up to the Fermi level provides the ICOHP (Integrated COHP) value, an index of net bond strength. A more negative ICOHP value indicates a stronger bond between the atoms [S6]. COHP analysis is particularly valuable for catalysis as it reveals how adsorbates bind to catalyst surfaces and whether orbital interactions stabilise or destabilise the binding. Specifically, it determines the occupancy of bonding versus antibonding orbitals involved in adsorption. This enables correlation between electronic structure and catalytic activity, since effective catalysts require an optimal

* esmail.doustkhah@istinye.edu.tr
† h.assadi.2008@ieee.org

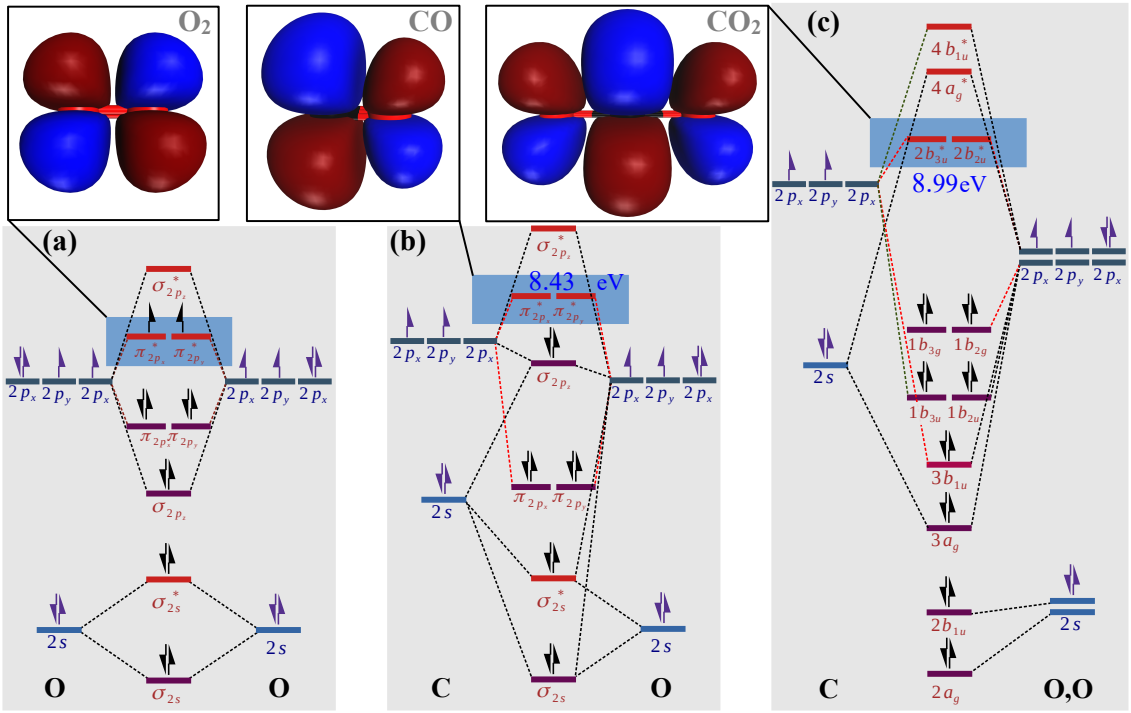


Figure S1. The arrangement of the molecular orbitals for the $O_2$, CO and $CO_2$ molecules is given in (a), (b) and (c), respectively. The lowest empty (or partially empty) orbitals available for accepting electrons during catalytic reactions are marked in blue, and their eigenvalues relative to the highest occupied molecular orbitals are given. These quantum molecular calculations were conducted using the Gaussian code [S5] and computational settings equivalent to the supercell calculations reported in the Computational Settings.

balance: strong reactant binding whilst avoiding excessive product stabilisation.

To use COHP analysis for further investigating the CO oxidation process, we studied the adsorption of CO, $O_2$, $CO_2$ and (CO + $O_2$) on the Au(111) surface. The surface was constructed by cleaving a $2 \times 2 \times 1$ Au supercell orthogonal to the (111) surface. The surface was two layers deep, with the positions of the bottom Au layer being constrained. Multiple starting configurations were examined and optimised, and the most stable ones were reported. Structural stability at room temperature was verified using *ab initio* molecular dynamics under canonical ensemble with Nosé-Hoover thermostat [S7] at 300 K for 10 ps (0.25 fs timesteps). Configurations remained stable aside from thermal motion. Finally, COHP analysis was performed using LOBSTER code [S8] with a very tight $k$-point mesh of $23 \times 23 \times 1$.

Using Spin-resolved COHP analysis of CO, $O_2$, CO + $O_2$ and $CO_2$ molecules on the Au's (111) surface, here we examine a possible pathway for CO oxidation ($CO + \frac{1}{2} O_2 \longrightarrow CO_2$). Figure S2 shows the adsorption of the isolated CO molecule on the Au surface, with the C end stabilising closer to the Au surface. The C−Au interaction, based on COHP analysis, is dominated by occupied bonding states below the Fermi level ($\sim -4$ eV) with minimal occupied antibonding weight, predicting Au−C chemisorption. The integrated −COHP, −ICOHP, value is about 0.037 $e$/bond. Figure S3 shows the adsorption of an isolated $O_2$ molecule on the Au surface, stabilised with both $O_2$ atoms bonding to the Au surface. Both O−Au interactions are dominated by occupied bonding states below the Fermi level at $\sim -15$, $\sim -8$ and $\sim -6$ eV. The combined −ICOHP is 0.623 $e$/bond, indicating a bond an order of magnitude stronger than that of CO.

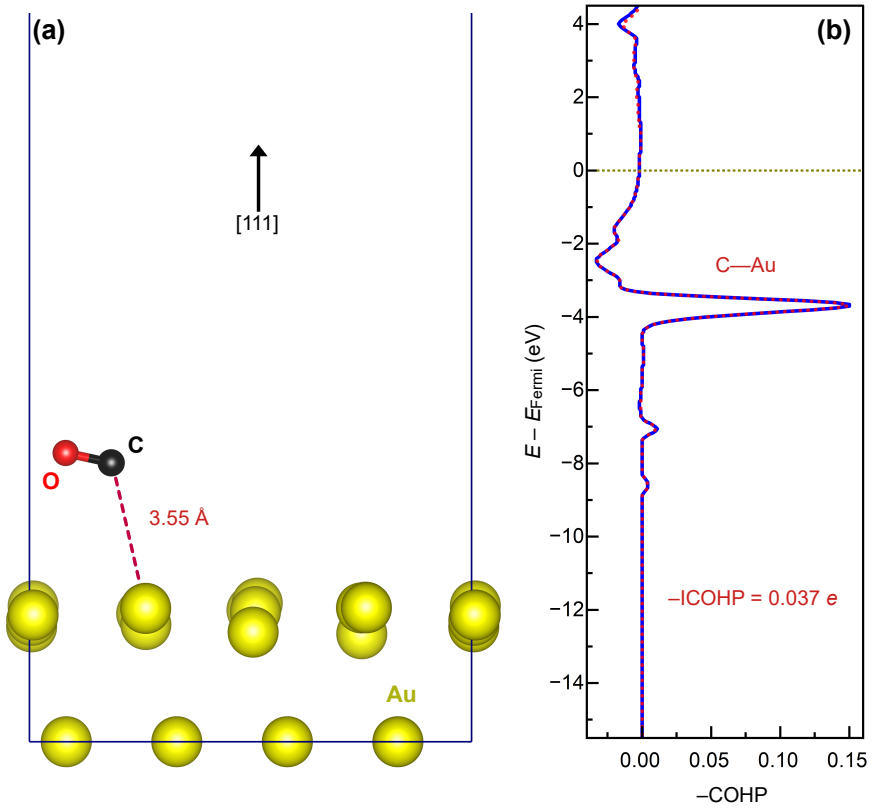


Figure S2. (a) Optimised structure of CO adsorption on the Au(111) surface. (b) −COHP plot for the C−Au interaction. Blue and red curves denote the spin-up and spin-down channels, which are degenerate in this case.

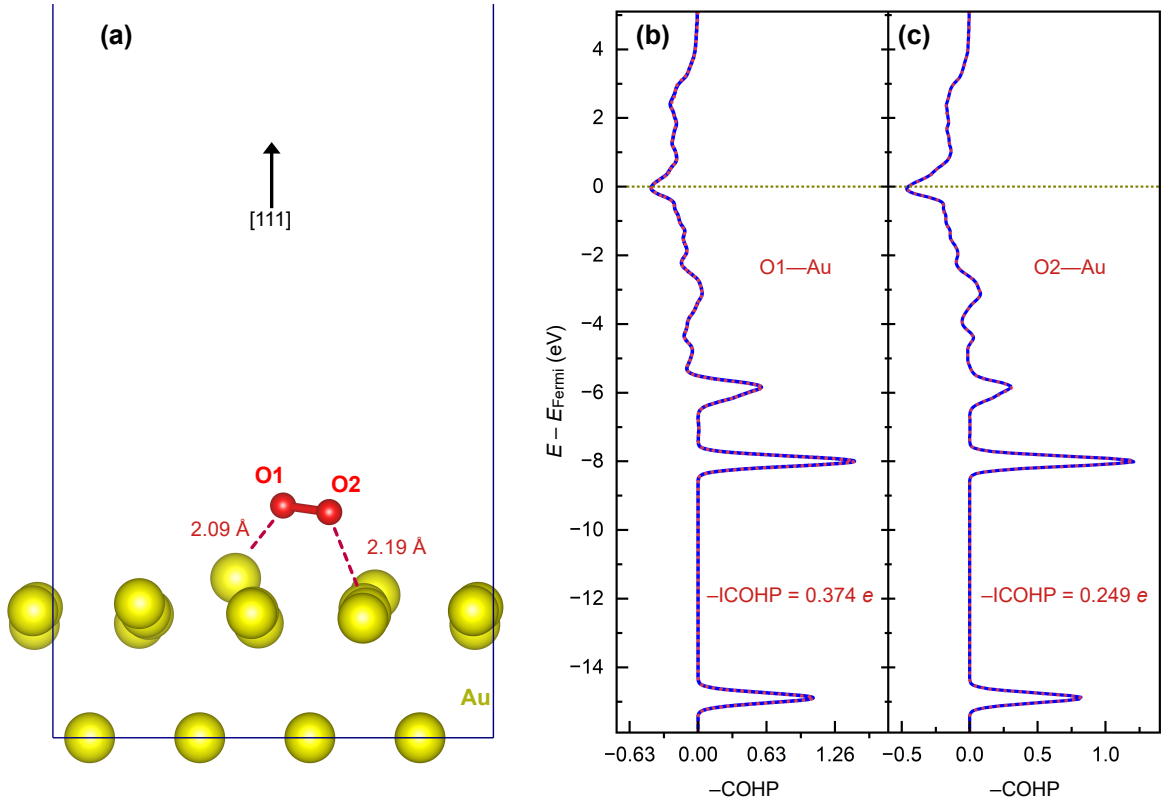


Figure S3. (a) Optimised structure of $O_2$ adsorption on the Au(111) surface. (b) and (c) −COHP plot for the two O−Au interactions. The two oxygen atoms in the adsorbed $O_2$ molecule are labelled O1 and O2. As O1 and O2 relax to different distances from their nearest Au atoms, their integrated −COHPs differ slightly. Blue and red curves denote the spin-up and spin-down channels, which are degenerate in this case.

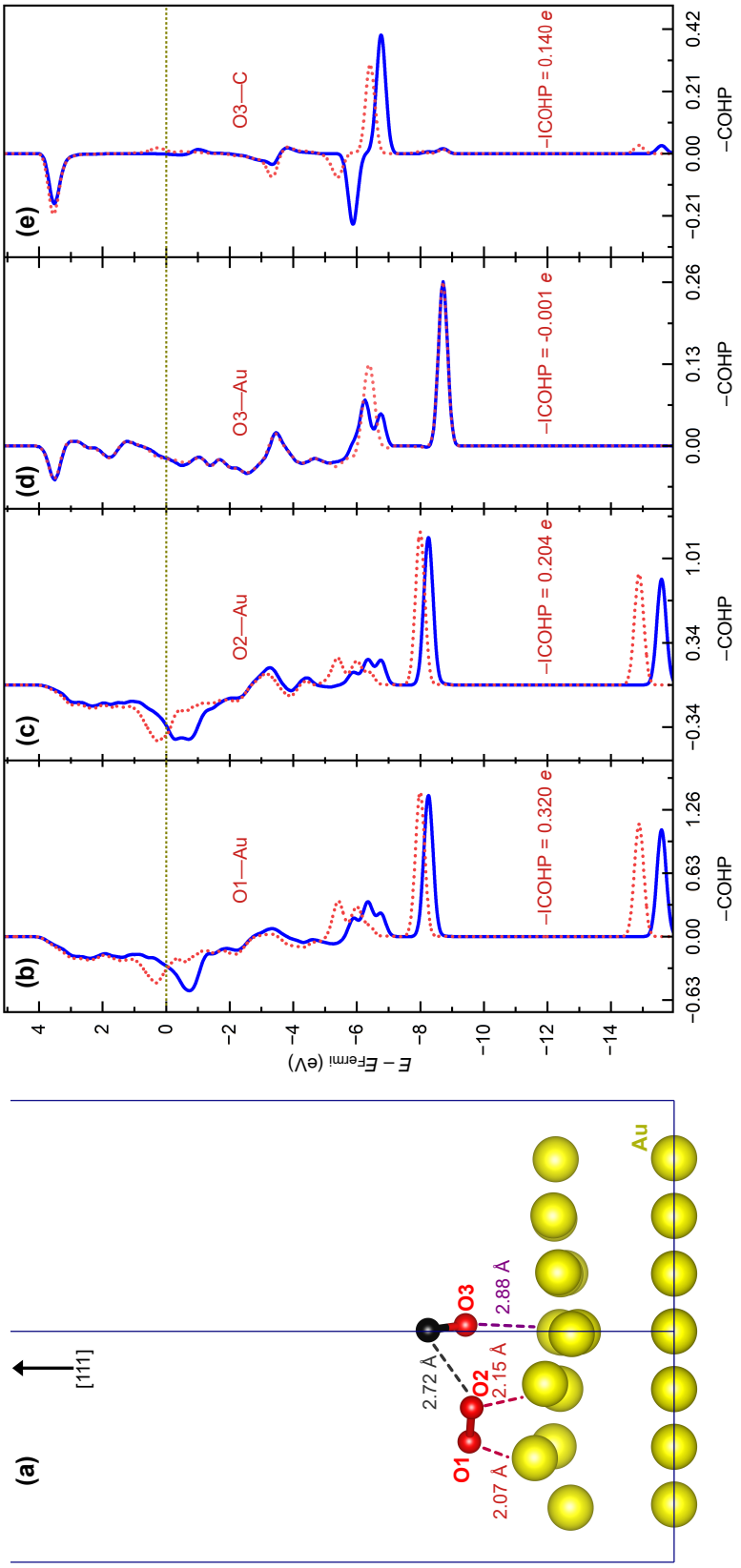


Figure S4. (a) Optimised structure of $O_2$ and CO co-adsorption on the Au(111) surface. (b, c) −COHP plots for the two O−Au interactions originating from the $O_2$ molecule. The oxygen atoms in adsorbed $O_2$ are labelled O1 and O2. As O1 and O2 relax to slightly different distances from their nearest Au atoms, their integrated −COHPs show minor variations. (d) −COHP for the interaction between the CO oxygen (O3) and Au. (e) −COHP for the interaction between the CO carbon and the $O_2$ oxygen (O2). Blue and red curves denote the spin-up and spin-down channels in the COHP analysis.

Figure S4 illustrates the co-adsorption configuration of CO and $O_2$ molecules on the Au surface. Upon co-adsorption, the CO molecule reorients such that its oxygen atom (denoted O3) faces the Au surface, while its carbon atom points toward the $O_2$ molecule. The $O_2$ molecule, in contrast, largely retains the same configuration as in its isolated adsorption state. The combined −ICOHP for the $O_2$ molecule (its atoms denoted as O1 and O2) is 0.524 $e$/bond. indicating a slightly weaker adsorption compared to the isolated $O_2$ molecule. For CO, the combined −ICOHP is 0.139 $e$/bond, which is about three folds larger than that of isolated CO (0.037 $e$/bond), exculsively promoted by the CO's attraction to the $O_2$ molecule on the Au(111) surface.

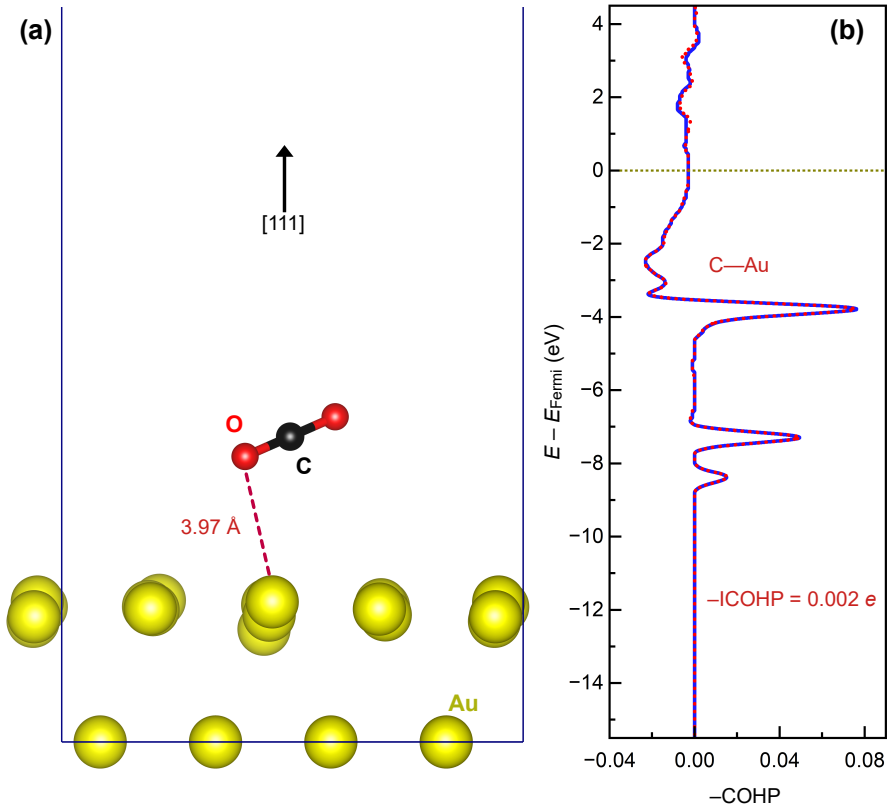


Figure S5. (a) The optimised structure of $CO_2$ molecule adsorption on Au(111) surface. (b) One of the $CO_2$'s oxygen atoms bonds to the Au surface, for which the −COHP graph is presented. The blue and red lines represent spin-up and spin-down curves, which in this case are degenerate.

Figure S5 shows the adsorption of the isolated $CO_2$ molecule on the Au surface, with one of the O ends stabilising closer to the Au surface. According to the COHP analysis, the interaction between O and Au is characterised by several occupied bonding peaks appearing below the Fermi level (around $\sim -4$, $\sim -7$, and $\sim -9$ eV), and an antibonding tail below the Fermi level, consistent with weak adsorption. The corresponding integrated –COHP (–ICOHP) value is 0.002 $e$/bond, which is the smallest among the investigated molecules.

From the simulations, it can be inferred that in the isolated state, $O_2$ exhibits a stronger interaction with the Au surface than either CO or $CO_2$. In the presence of pre-adsorbed $O_2$, however, the CO−Au interaction becomes significantly enhanced. These observations suggest that CO oxidation on Au surfaces is initiated by O adsorption, which subsequently promotes CO adsorption and activation. The resulting $CO_2$ species exhibits a substantially weaker interaction with the surface, facilitating its desorption and completing the catalytic cycle. By elucidating systematic molecular adsorption trends, this work provides additional perspective that may assist in interpreting earlier computational studies on small-molecule adsorption at metallic interfaces [S9, S10].

[S1] M. Haruta, T. Kobayashi, H. Sano, and N. Yamada, Novel gold catalysts for the oxidation of carbon monoxide at a temperature far below 0 °C, Chem. Lett. **16**, 405 (2006).

[S2] D. Widmann and R. J. Behm, Activation of molecular oxygen and the nature of the active oxygen species for CO oxidation on oxide supported Au catalysts, Acc. Chem. Res. **47**, 740 (2014).

[S3] M. Farnesi Camellone and D. Marx, Nature and role of activated molecular oxygen species at the gold/titania interface in the selective oxidation of alcohols, J. Phys. Chem. C **118**, 20989 (2014).
[S4] M. L. Kimble, N. A. Moore, G. E. Johnson, J. Castleman, A. W., C. Bürgel, R. Mitrić, and V. Bonačić-Koutecký, Joint experimental and theoretical investigations of the reactivity of $Au_2O_n^-$ and $Au_3O_n^-$ ($n = 1$–$5$) with carbon monoxide, J. Chem. Phys. **125**, 204311 (2006).
[S5] M. e. Frisch, G. Trucks, H. B. Schlegel, G. Scuseria, M. Robb, J. Cheeseman, G. Scalmani, V. Barone, G. Petersson, H. Nakatsuji, *et al.*, Gaussian 16 (2016).
[S6] S. Steinberg and R. Dronskowski, The crystal orbital Hamilton population (COHP) method as a tool to visualize and analyze chemical bonding in intermetallic compounds, Crystals **8**, 225 (2018).
[S7] W. G. Hoover, Canonical dynamics: Equilibrium phase-space distributions, Phys. Rev. A **31**, 1695 (1985).
[S8] S. Maintz, V. L. Deringer, A. L. Tchougréeff, and R. Dronskowski, LOBSTER: A tool to extract chemical bonding from plane-wave based DFT, J. Comput. Chem. **37**, 1030 (2016).
[S9] K. W. Qadir, M. D. Mohammadi, N. J. Ridha, and H. Y. Abdullah, Determining the binding mechanism of $B_{12}N_{12}$(Zn) with $CH_4$, CO, $CO_2$, $H_2O$, $N_2$, $NH_3$, NO, $NO_2$, $O_2$, and $SO_2$ gases, Microporous Mesoporous Mater. **379**, 113289 (2024).
[S10] K. W. Qadir, M. Doust Mohammadi, and H. Y. Abdullah, Adsorption mechanism of CO, $CO_2$, NO, $NO_2$, and $SO_2$ gases onto AlNNT$(m, n)_k$, ($m = 5, 7$; $n = 0, 5, 7$; $k = 3 \sim 9$), Mater. Sci. Semicond. Process. **185**, 108973 (2025).